Magnetron sputtered WS_2; optical and structural analysis

Y Koçak[1], Y Akaltun[2] and Emre Gür[1]

[1]Department of Physics, Faculty of Science, Atatürk University, 25240 Erzurum, Turkey
[2]Department of Electric Electronic Engineering, Erzincan, Turkey

E- mail: emregur@atauni.edu.tr

Abstract. Remarkable properties of graphene have renewed interest in inorganic, Transition Metal Dichalgogenits (TMDC) due to unique electronic and optical properties. TMDCs such as MoS_2, $MoSe_2$, WS_2 and WSe_2 have sizable bandgaps that change from indirect to direct in single layers, allowing applications such as solar cells, transistors, photodetectors and electroluminescent devices in which the graphene is not actively used. So, fabrication and analysis of these films are important for new generation devices. In this work, polycrystalline WS_2 films were grown by radio frequency magnetron sputtering (RFMS) on different substrates like n-Si(100), n-Si(111), p-Si(100), glass and fused silica. Structural, morphological, optical and electrical properties were investigated as a function of film thickness and RF power. From XRD analysis, signals from planes of (002), (100), (101), (110), (008) belong to the hegzagonal WS_2 were obtained. Raman spectra of the WS_2 show that there are two dominant peaks at ~351 cm^{-1} (in-plane phonon mode) and ~417cm^{-1} (out-of-plane phonon mode). XPS analysis of the films has shown that binding energy and the intensity of tungsten 4f shells shifts by depending on the depth of the films which might be due to the well-known preferential sputtering.

1. Introduction

Unique optical and electrical properties of 2D materials permit many important device applications. One of the most well-known 2D material graphene attracts attention for semiconductor device applications due to its strong interaction with photons in a wide energy range and its high carrier mobility, in a broad wavelength range [1-3]. However, field effect transistors produced from graphene cannot be effectively switched off and have low on/off switch ratios due to lack of bandgap [4]. This brings up the importance of other 2D materials. Many other 2D materials are known such as TMDCs (transition metal dicalcogenides), MX_2, M;transition metal (Mo, W, i.e) and X; chalcogenide (S, Se, i.e) [4, 5]. TMDC materials such as MoS2 and WS2 are covalently bonded to six chalcogenide neighbors within the same plane, but weakly linked to sheets above and below by van der Waals force. The layers are stacked along the c-axis. If the thin films grown with the c-axis parallel to substrate, i.e. the X-M-X layers are perpendicular to the substrate, they will referred to as " l l c ". The "⊥c" orientation has the advantage of photovoltaic materials, with c axis perpendicular and layers parallel to the substrate [6].

Important properties of 2D materials are [2]; 1) their surfaces are naturally self-passivated without any dangling bonds, making the integration of 2D materials with photonic structures easy, for example such as waveguides and cavities. 2) It is possible to raise vertical hetero-structures using different 2D materials without the conventional lattice mismatch, due to sheets with different lattice constants in hetero-structures are only weakly bonded by van der Waals force as in layered materials. 3) Even if the thin films exist atomically thin, many 2D materials interact with light strongly. For example a single layer tungsten disulfide (WS_2) absorbs roughly %10 at exitonic resonances (615nm) [7]. 4) 2D materials can cover a very wide electromagnetic spectrum, since their diverse electronic properties [2].

In this paper, WS_2 thin films grown by sputtering are investigated depending on the film thickness and substrate. The structural analysis has been performed by using X-ray diffraction (XRD). Raman spectroscopy used to the phonon modes that can provide a fingerprint for WS_2 thin films. X-ray photoelectron spectroscopy (XPS) was used in order to investigate the elemental analysis together with the depth profile analysis.

2. Experimental Produce

WS2 thin films were deposited by Radio Frequency Magnetron Sputtering (RFMS), using %99.99 WS_2 target. Substrates were chemically cleaned prior to the insertion in the vacuum chamber. Base pressure of $2x10^{-7}$ Torr was reached in the sputtering chamber before the growth process. Growth pressure was 8.6mT. Five different substrates were put in the chamber in order to investigate the substrate effect on the WS2 films. The substrates temperature was 350 ^{0}C during the deposition. Details of the deposition parameters are summarized in table 1.

Table 1. Parameters of sputtering system

Target (purity)	WS_2 (99.99%)
Target diameter	2 inc
Target to substrate distance	80 mm
Base pressure	2×10^{-7} torr
Sputtering pressure	8.6 mtorr
Substrate temperature	350 ^{O}C
Substrates	Si(100), Si(111), fused silica, quartz, glass

Structure of the thin films was studied by x-ray diffraction (XRD) with Empyrean, PANalytical with Cu K_α radiation. The measurements were performed at grazing incidence angle of 0.5 ^{o} degree. Further evidence for composition of the grown thin films was obtained using XPS which was performed with a Thermo Scientific K-Alpha–Monochromated high-performance XPS spectrometer. Raman measurements were conducted with Ar+ laser wavelength of 514.5 nm with a CCD camera attached to the 1 m long monochromotor.

3. Results and discussion

A comparison of the XRD profiles of WS_2 thin films grown in different RF power is illustrated in Fig. 1. Polycristalline nature of thin films is observed in multiple peaks in the XRD spectra. Three distinct peak clearly observed in the figure. The first one appeared around 13.24^0 degree which is belong to the (002) plane. Second peak observed in the XRD spectra of the thin films attributed to the combined (10*l*) (*l is* 0,1,2..), third peak which is (103) observed only in the thin film grown at 6 WRF power38.08 degree and forth peak is observed at 60.9 degree which is (11*l*). Dominant crystal orientation in the grown thin films has changed by changing the RF power from (002) to (10l) as shown in Fig. 1. The degree of preferred orientation, which can be inferred from the peak heigh of the (002) peak is dramatically decreased by increasing RF power in the growth process. FWHM (full widh half maximum) of the all peaks observed in the XRD spectra given aboveshows that FWHM inreases while increasing of RF power (i.e. FWHMs of (002) and (112) peaks are increasing from 3.30 to 6.31 and from 2.35 to 2.84 respectively but FWHMs of (100)+(101) peak are decreasing from 2.24 to 1.68, while RF power increased).

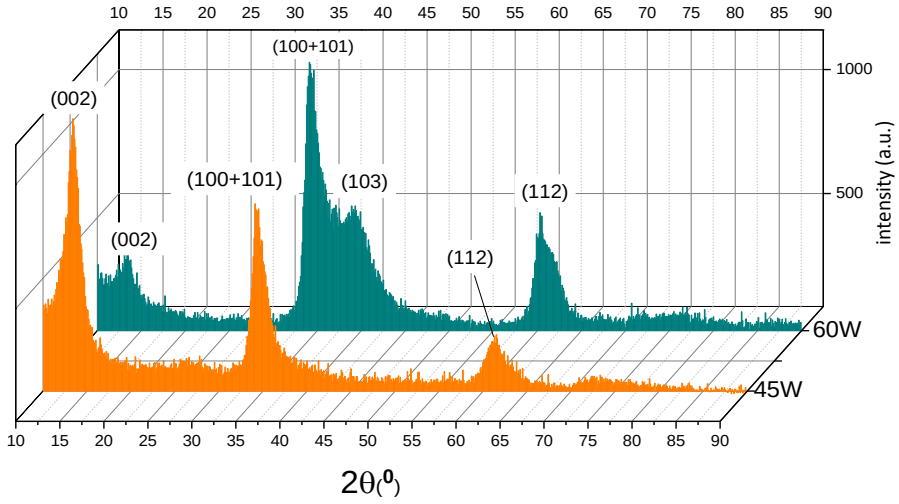

Fig. 1. XRD-patterns in different RF power of WS2 films on n-Si(111) substrate.

This might be due to the observation of some extra peaks, namely (103), plane as observed in the thin film grown at 60W. Also, (002), (112) and combined (100)+(101) peaks are slightly has shifted smaller angles as a function of RF power. If diffraction occurs off of the horizontal planes (tensile strain), and the Bragg peak shifts to higher angle as the interplanar spacing decreases [8, 9]. Then it can be confirm that the (002), combine (101) + (101) and (112) plane exposure to compresive strain.
Raman Spectroscopy was used to characterize the samples' structural quality and vibrational properties. Since it is non-devastating technique and it is widely used to characterize the structural and electronic properties of monolayer materials such as graphene, WS_2 and MoS_2 [10-12]. To reason out this observation we fitted the Raman peaks using a Voigh function and positions E^1_{2g} and A_{1g} modes depending on the type of the substrate. The clear observation of the raman modes indicates good quality of the material. The Raman spectra for the various substrate (p-Si(100), n-Si(111) and fused silica) in 310nm WS_2 thin films are shown in Fig. 2. It is confirmed that the WS_2 exhibit first order modes at wavenumber of 348 cm^{-1} and 418 cm^{-1} separated by about 70 cm^{-1}, corresponding to the E^1_{2g} and A_{1g} modes from in plane and out-of plane vibrations, respectively.

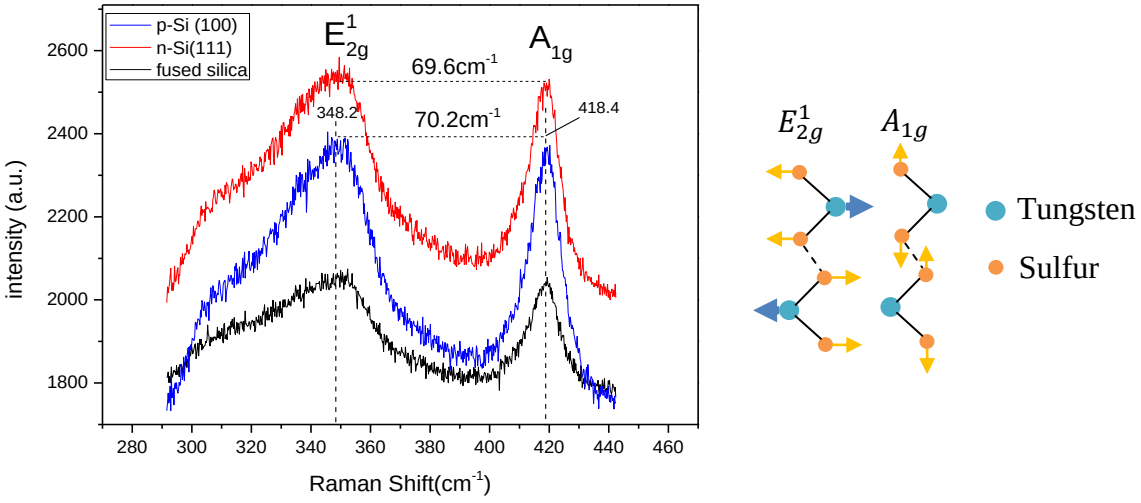

Fig. 2. Room-temperature Raman spectra from a monolayer WS2 region; 310nm thickness of WS_2 thin films on various substrate (45W RF Power).

The peak of E_{2g}^1 mode is broad due to consisting of another mode so called 2LA(M) (second-order longitudinal acoustic mode) [11, 13, 14]. In generally, 2LA(M) peak which matches in energy with the density of states absorption peak, is prevalent as a small left portion of the E_{2g}^1 peak [14]. small changes observed depending on the substrate type in Raman modes. This might be due to the different strain in which the grown WS_2 thin films are subjected to. In addition Raman peak shifts are showing a trend to decrease in frequency of the optical E_{2g}^1 phonon mode and an increase in frequency of A_{1g} phonon mode with increasing thickness of the thin films (Fig. 2.). These variations in the Raman frequency of the A_{1g} and E^1_{2g} modes depending on the different substrate can be explained by weak interlayer substrate can be explained by weak interactions and the reduced long-range Coulomb interaction between the effective charges caused by an increase in the dielectric screening, respectively [13, 15, 16]. No raman signal corresponding to the WO_3 has been observed.
XPS measurements performed in order to find out the concentration of the elements. As shown in Fig. 3, XPS survey spectrum of WS_2 shows that only C, O, W and S is observed all of the films in. To identify the chemical composition of WS_2 thin films, XPS was used to measure the binding energy of W and S as well as carbon and oxygen.

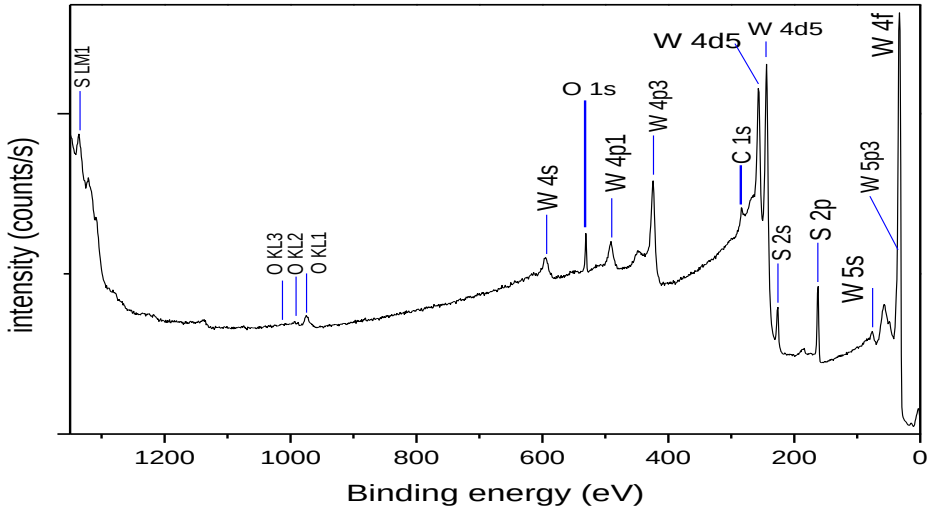

Fig. 3. XPS survey spectrum of WS_2 thin film after 100s etched.

Depth resolved XPS measuements were used to understand the elemental profile of W and S. Ar gun was used to achive etching procesXPS data was acquired 120s of sputter between every measurement. The characteristic W4f and S2p XPS spectrum of WS_2 thin film is shown in figure 4.The binding energy profile for $W4f_{7/2}$ and $W4f_{5/2}$ is represented by two peak at 31.5eV and 33.8eV, respectively, corresponding to W in WS_2 [17-19], after the film is etched for the first 120s. the W 4f spectrum has consisted of 4 peaks for the last three XPS measuments (see fig. 4.a). The appeared peaks shows a shift to higher binding energy values i.e. 35.7eV and 37.6 which might be corresponding to tungsten in WO_3 (W^{6+}) [17, 20] While $W4f_{7/2}$ peak intensity of WS_2 decreases with the depth profile, possible observed peaks belong to the WO_3 starts to increase, as shown in Fig. 4. a. As shown in figure 4.d, the S2p spectrum is deconvoluted to a dublet consisting of $S2p_{3/2}$ and $S2p_{1/2}$ peaks centered at binding energy values of 161.88eV and 163.18eV which correspond to S^{2-} in WS_2.
In order to find the peak energy position of the W 4f belonging to WS_2, Lorentz function were used to fit observed data (see fig.4.c). Binding energy shifts has observed in 4f features as shown in the inset of figure 4c.

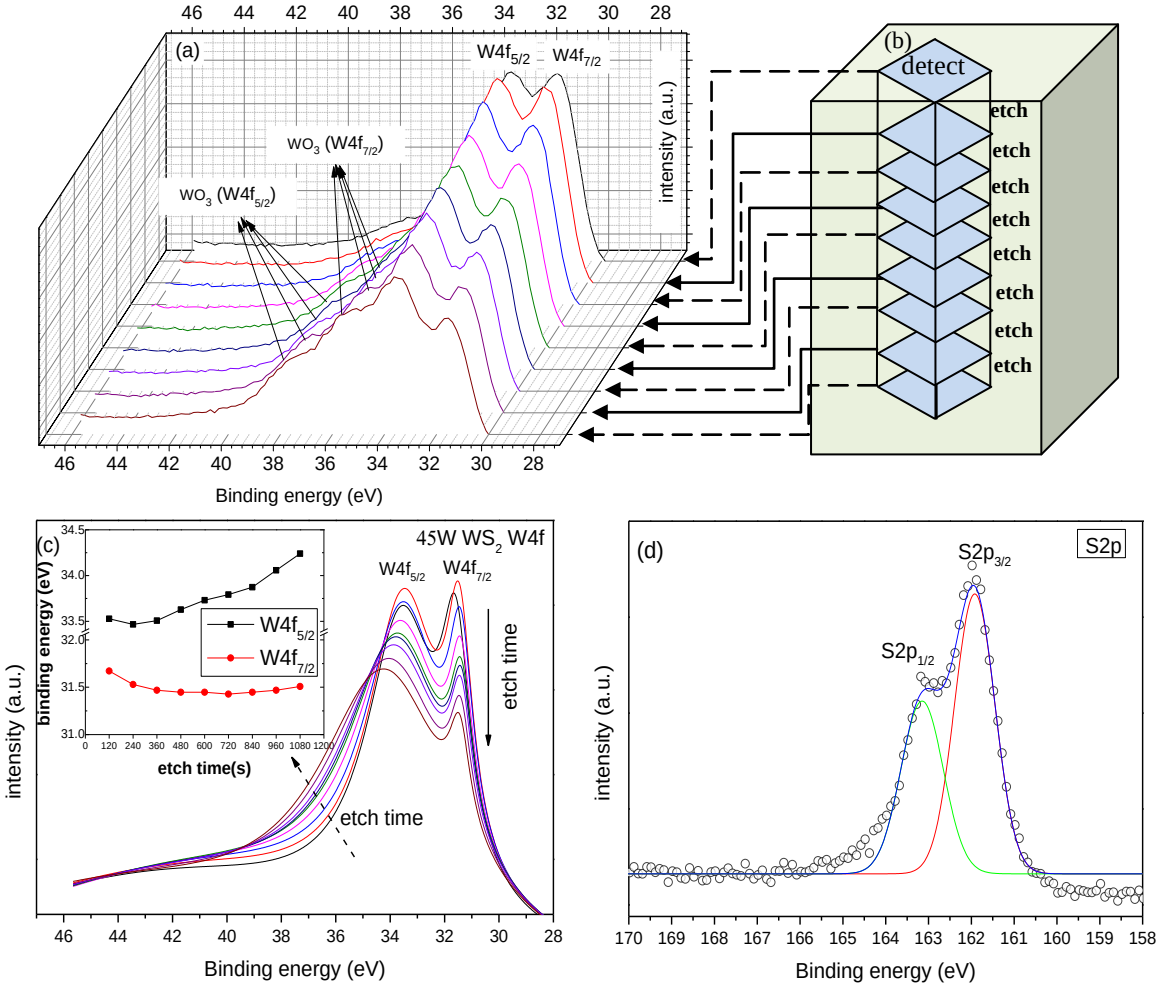

Fig. 4. XPS analysis of WS_2 thin film, a) $W4f_{7/2\text{-}5/2}$ b) Schematic illustration of grid zone in an XPS depth profile c) the Lorentz fit data graph of WS_2 thin film at fig 4.a and also shown is the binding shifts while the etch time is increasing (inset) d) S2p binding energy.

Figure 5 shows the UV visible absorption spectrum of WS_2 thin film.

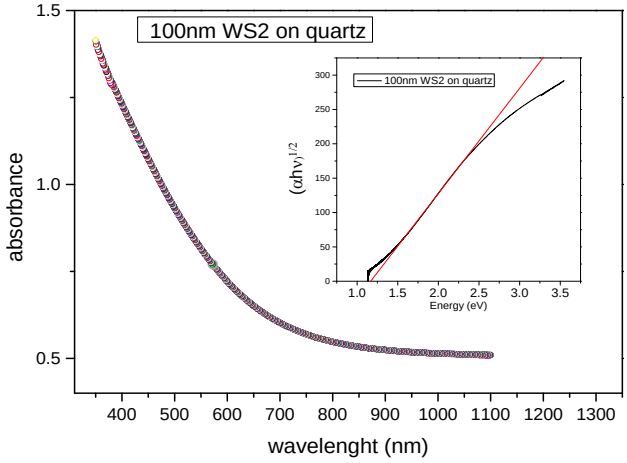

Fig. 5. Optical absorption of WS_2 thin film in a wavelength range of 350-1100 nm with an computed optical bandgap ~1.17 eV from the calculated at the lineer fit of optical absorbance plot data, as shown in the inset.

The figure inset shows the bandgap energy obtained from plotting the $(\alpha h\nu)^{1/2}$~$(h\nu-E_g)$ graph, where α is the absorption coefficient of the WS_2, $h\nu$ is the incident photon energy, and Eg is the optical bandgap. Bandgap energy of the WS_2 was obtained from the linear fit as shown in the inset of the figure 5 as 1.17 eV which is very close to the bulk indirect bandgap of the WS_2.

4. References

[1] Mak KF, Ju L, Wang F, Heinz TF, 2012. *Solid State Commun.*;**152**:1341-9.
[2] Xia F, Wang H, Xiao D, Dubey M, Ramasubramaniam A, 2014 *Nature Photonics*.**8**:899-907.
[3] Xia F, Yan H, Avouris P, 2013 *Proceedings of the IEEE*.**101**:1717-31.
[4] Wang QH, Kalantar-Zadeh K, Kis A, Coleman JN, Strano MS, 2012 *Nature nanotechnology*.**7**:699-712.
[5] Fiori G, Bonaccorso F, Iannaccone G, Palacios T, Neumaier D, Seabaugh A, et al., 2014 *Nature nanotechnology*.**9**:768-79.
[6] Martin-Litas I, Vinatier P, Levasseur A, Dupin J, Gonbeau D, Weill F, 2002 *Thin Solid Films*.**416**:1-9.
[7] Eda G, Maier SA, 2013 *Acs Nano*.**7**:5660-5.
[8] Regula M, Ballif C, Moser J, Levy F, 1996 *Thin Solid Films*.**280**:67-75.
[9] Hashmi S. 2014 Comprehensive Materials Processing: Newnes.
[10] Calizo I, Balandin A, Bao W, Miao F, Lau C, 2007 *Nano Lett.*;**7**:2645-9.
[11] Su L, Yu Y, Cao L, Zhang Y, 2015 *Nano Research*.**8**:2686-97.
[12] Su L, Zhang Y, Yu Y, Cao L, 2014 *Nanoscale*.**6**:4920-7.
[13] Berkdemir A, Gutiérrez HR, Botello-Méndez AR, Perea-López N, Elías AL, Chia C-I, et al., 2013. *Scientific reports*.**3**:
[14] Zhao W, Ghorannevis Z, Amara KK, Pang JR, Toh M, Zhang X, et al., 2013 *Nanoscale*.**5**:9677-83.
[15] Molina-Sanchez A, Wirtz L, 2011 *Physical Review B*.**84**:155413.
[16] Song J-G, Park J, Lee W, Choi T, Jung H, Lee CW, et al., 2013 *ACS nano*.**7**:11333-40.
[17] Deepthi B, Barshilia HC, Rajam K, Konchady MS, Pai DM, Sankar J, et al., 2010 *Surf. Coat. Technol.*;**205**:565-74.
[18] Sundberg J, Lindblad R, Gorgoi M, Rensmo H, Jansson U, Lindblad A, 2014 *Appl. Surf. Sci.*;**305**:203-13.
[19] Yin G, Huang P, Yu Z, He D, Tu J, 2006 *Tribology Letters*.**22**:37-43.
[20] Wong K, Lu X, Cotter J, Eadie D, Wong P, Mitchell K, 2008 *Wear*.**264**:526-34.

Acknowledgments

We appreciate Hasan Feyzi Budak for the XRD measurements This project was supported by Atatürk University Scientific Resarch Project Unit under contract No: 2015/343. We would like to thank to Enver Kahveci for the XPS measurements. We are thankful to Prof. Dr. Atilla Aydınlı for discussion on the Raman measurements.